



**Chapman Conference on Space Weather:
Progress and Challenges in Research and
Applications
Bellevue Biltmore Resort and Spa
Clearwater, Florida
March 20-24, 2000**

**Relativistic Electron Flux Limits
from GPS Satellite Observations**

Reiner H. W. Friedel, Geoffrey D. Reeves
LOS ALAMOS NATIONAL LABORATORY,
LOS ALAMOS, NEW MEXICO, USA



Sebastien Bourdarie
CERT-ONERA, 2 AVENUE EDOUARD BELIN,
TOULOUSE, 31055 FRANCE



Michel Tuszewski, Tom Cayton
LOS ALAMOS NATIONAL LABORATORY,
LOS ALAMOS, NEW MEXICO, USA



Contents



- A. Abstract
- B. Satellites
- C. Instrument
- D. Motivation – NS24 observations
- E. Kennel-Petschek limit
- F. Observations – NS33 energies
- G. Flux Limit Energy dependence
- H. Observations – NS33 LE1 L-ranges
 - I. Flux Limit L dependence
- J. Conclusion



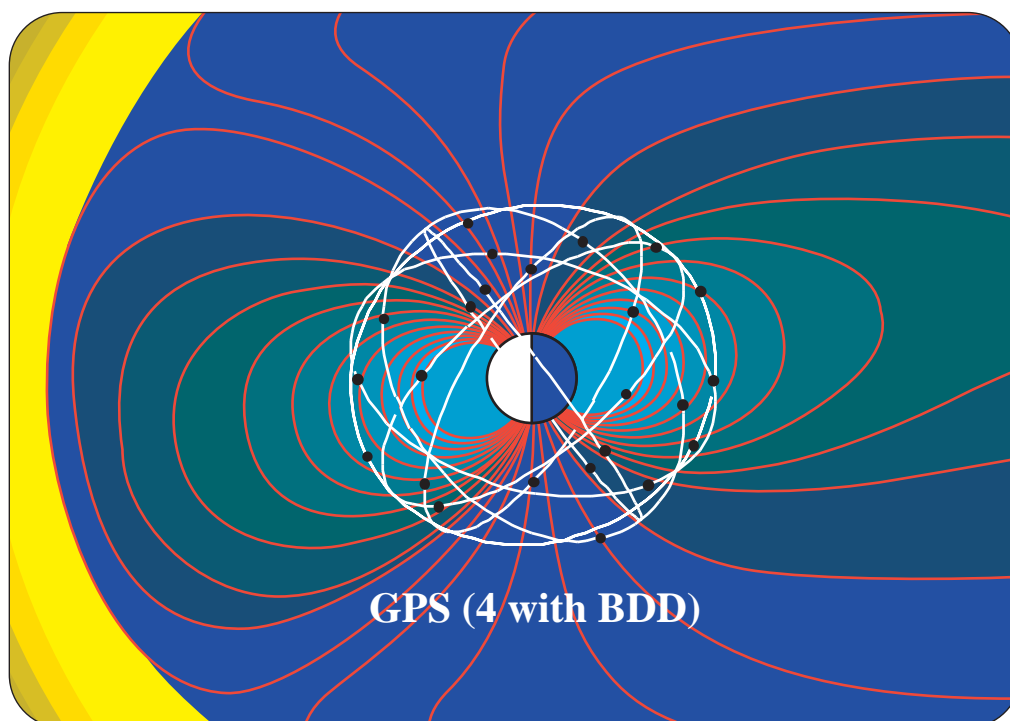
A. Abstract

Since 1990, up to 5 Global Positioning System (GPS) satellites provide omni directional electron flux estimates in the range 0.2–10 MeV with BDD-II dosimeters. The orbits of these satellites are circular with an altitude of about 20,000 km and an inclination of 55 degrees. As such, they pass through the peak intensity region of the radiation belts twice per 12 hour orbit. The instantaneous (every 96 s) electron fluxes of various energy channels were examined from 1991 to 1997. One interesting observation that emerged is that there seem to be well-defined flux upper bounds. These maximum flux values appear to depend on electron energy, on geomagnetic latitude, and on solar activity. The goal of this study is to understand the cause(s) of these apparent flux limits. The maximum flux is about $10^7 \text{ cm}^{-2}\text{s}^{-1}\text{sr}^{-1}$ at $L = 4.5$ for electrons with energy greater than 0.2 MeV. This limit is comparable to the Kennel-Petschek prediction based on weak pitch angle diffusion. Curiously, strong pitch angle diffusion associated with large magnetic storms would be expected to produce significantly higher flux levels, but these are not observed. There is also evidence from the data that instrumental effects such as electronics dead-time and pile-up may be involved in some of the above apparent flux limits. These instrumental effects will be analyzed.

B Satellites



- The GPS constellation:
24 satellites with circular orbits (radius $4.2 R_E$, 55° inclination, 12 hour period, $L : 4 \rightarrow 12$ in 3 hours)



- GPS with particle detectors:
Since 1990, up to 5 Global Positioning System (GPS) satellites provide omni-directional electron flux estimates in the range 0.2-10 MeV and omni-directional proton flux estimates in the range > 10 MeV, with BDD-II dosimeters.
- Extensively calibrated:
1 satellite (NS33) only with dosimeter calibrated

C Instrument



BDD II omni-directional electron dosimeter

- Provides 5 “low energy” channels (LE1 – LE5).
- Bow-tie calibration of these channels shows these to be INTEGRAL flux channels.

$$I(x) = \int_x^\infty J(x) dE, \quad J(x) = \int d\Omega$$

$$I(x) \text{ [cm}^{-2}\text{s}^{-1}] = \frac{C \text{ [s}^{-1}]}{G \text{ [cm}^{-2}]}$$

C is the count rate and G is the effective geometric factor.

- Bow tie results:

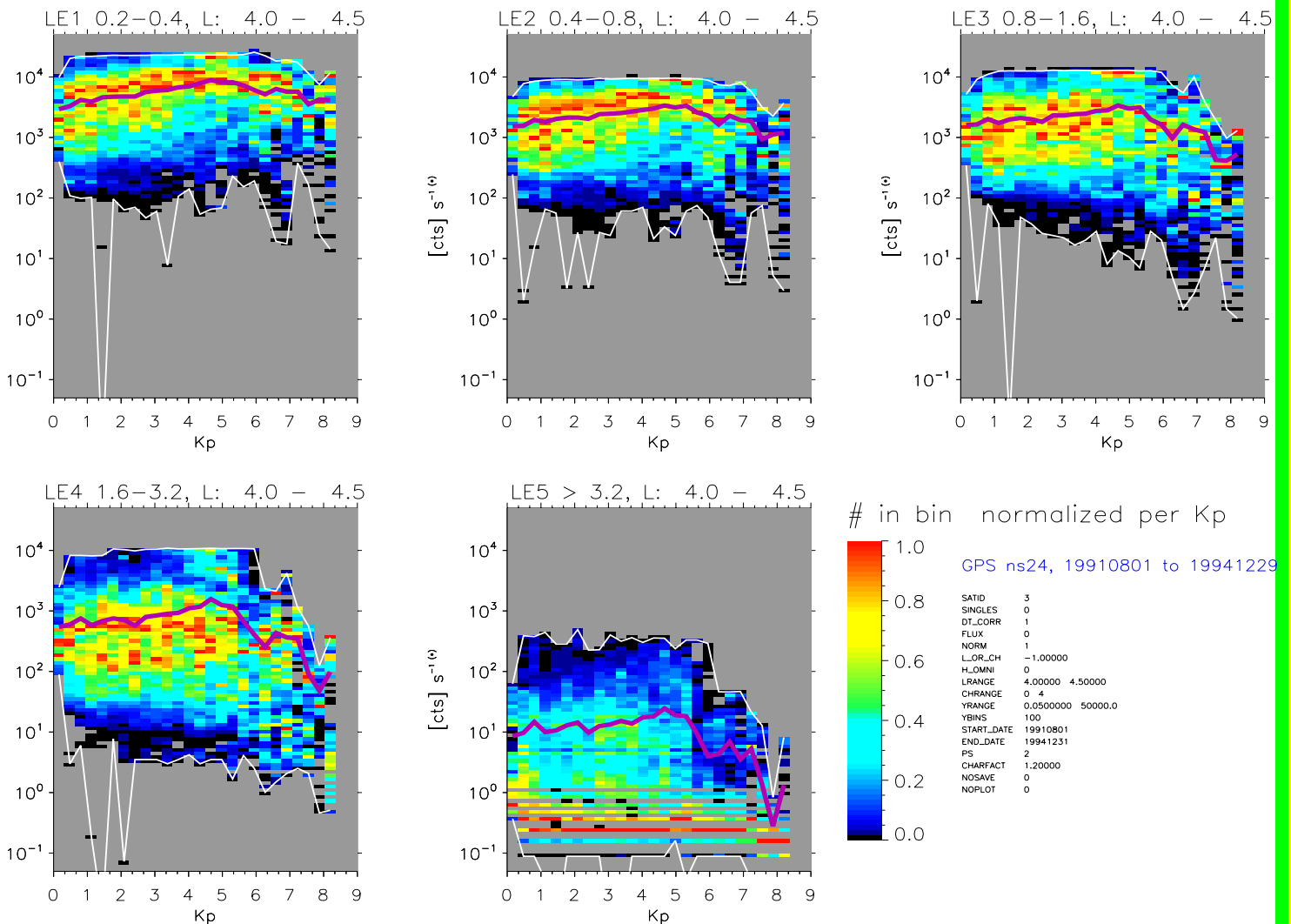
LE	1	2	3	4	5	units
G	1.07	0.72	1.06	1.24	0.48	$[10^{-4}\text{cm}^2]$
x	0.27	0.43	0.82	1.37	2.27	[MeV]
Ch	0.2–0.4	0.4–0.8	0.8–1.6	1.6–3.2	>3.2	[MeV]

x is the effective low energy cutoff of the channel and Ch are the theoretical design channel energies.

D.1 Motivation GPS NS24, Solar Max



Data from the raw count rate nominal energy channels showed clear apparent limits to the maximum count rates observed. NS24 has the best coverage of the GPS satellites. Data for 1991–1994 represents solar max.

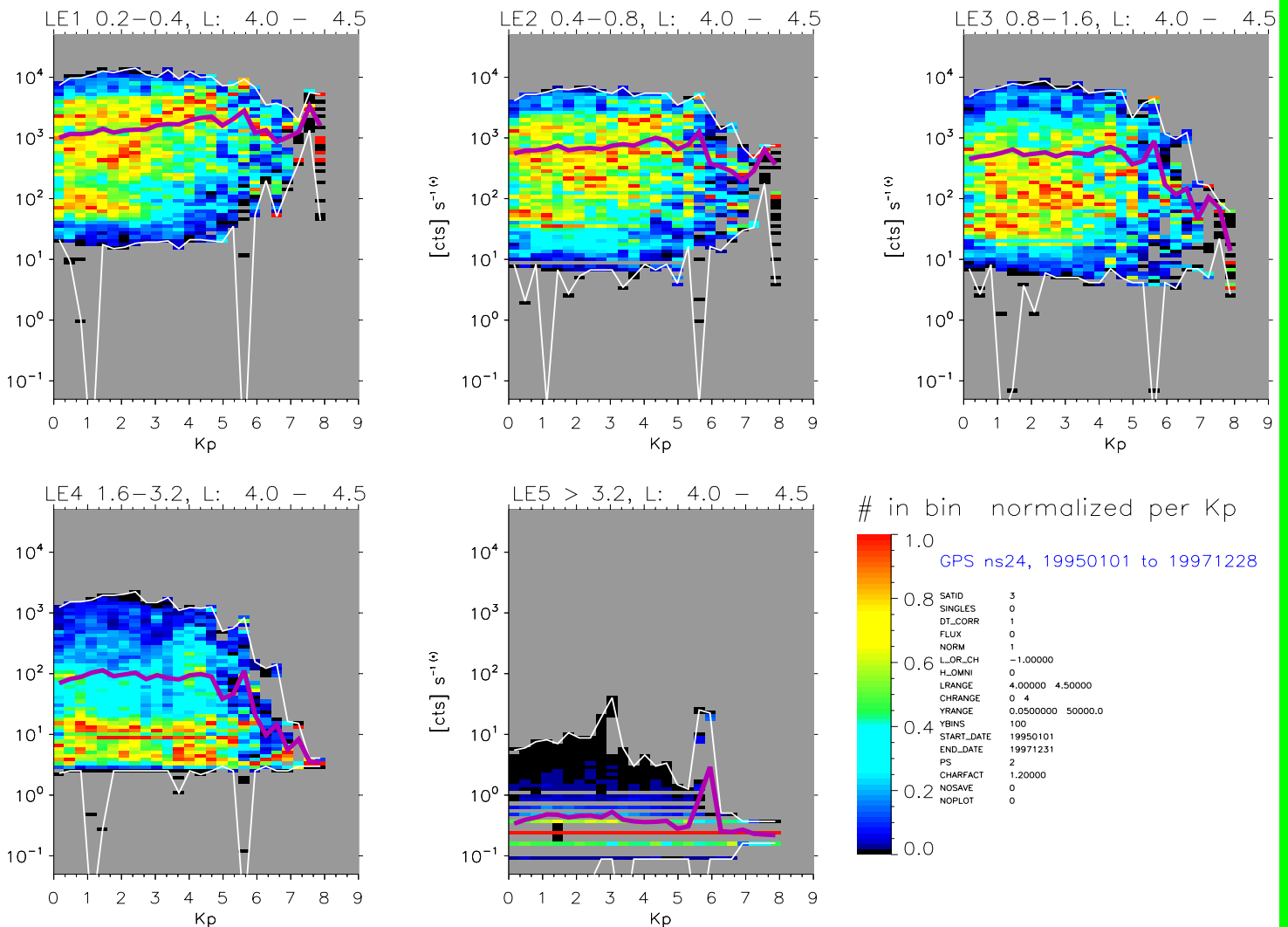


Data is normalized to the most frequently occurring flux in each Kp bin (purple curve). The white lines are the envelopes of the highest and lowest counts at each Kp.

D.2 Motivation GPS NS24, Solar Min



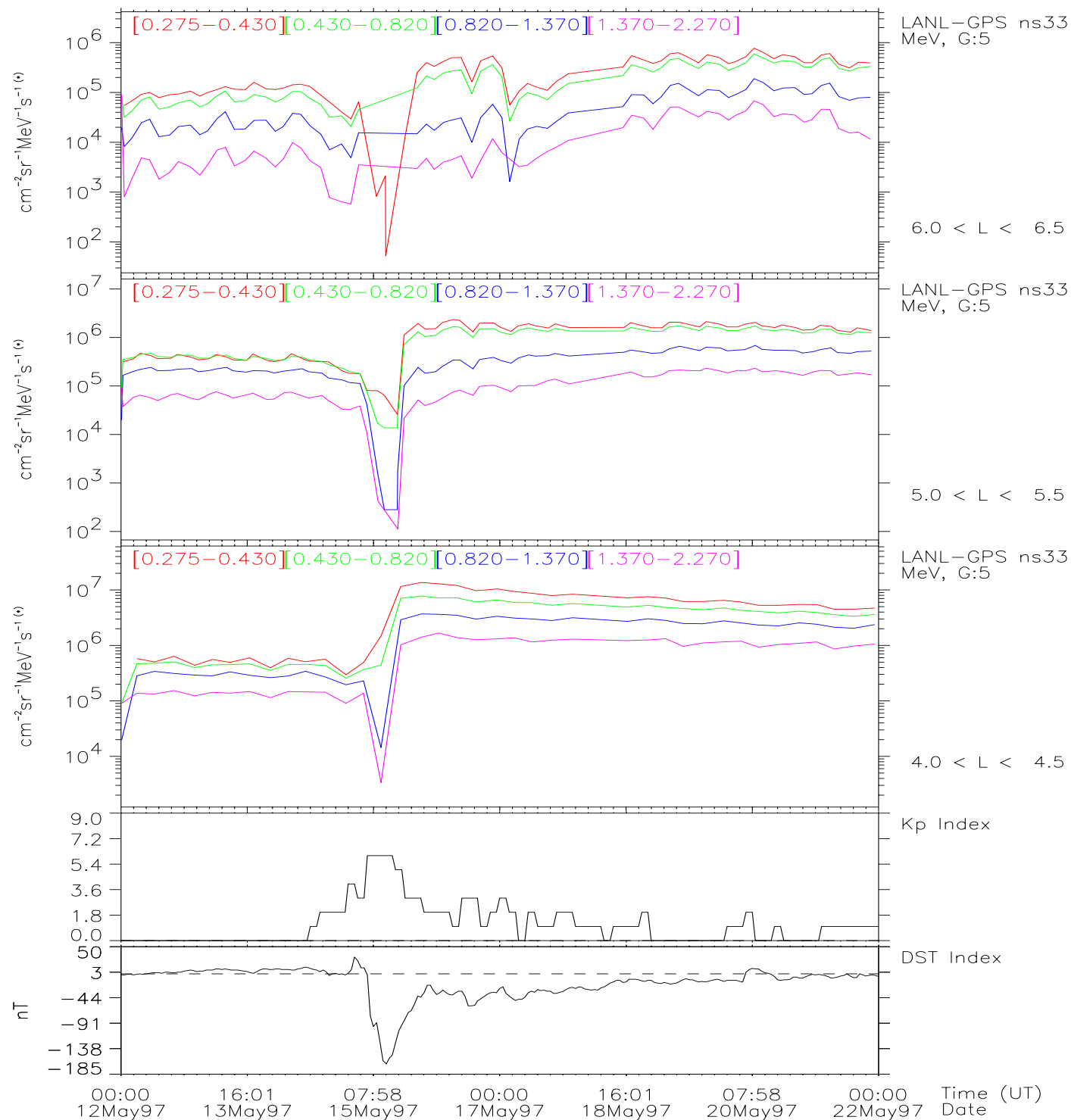
Data from the raw count rate nominal energy channels showed clear apparent limits to the maximum count rates observed. NS24 has the best coverage of the GPS satellites. Data for 1995–1997 represents solar min.



Data is normalized to the most frequently occurring flux in each Kp bin (purple curve). The white lines are the envelopes of the highest and lowest counts at each Kp.

D.3

Relativistic electron time lag vs. Kp



D.4 GPS NS24 Observations Discussion



- All energy channels show a flat, fixed maximum count rate which is independent of activity level (K_p). The counts have all been corrected for detector dead-time effects, which become important at count rates near 10^4 .
- The drop of the maximum count rate at the highest K_p is due to two effects:
 - A. Few events occur at these K_p levels
 - B. At the time of the highest activity levels, at storm onset, particles are lost due to adiabatic effects combined with drift shadowing by the magnetopause.

This effect is more pronounced at higher L-values (not shown here).

- Low energies show a general increase of average count rates with K_p
- Maximum count rates in general are higher at solar max.
- There seems to be a maximum in the occurrence rate of the maximum count rate for K_p values near 5. This effect is still under investigation.

E. Kennel-Petschek limit



Based on the classical paper: JGR 71, 1, 1966

- Wave growth + anisotropy leads to integral flux limit (where E^* is the integral flux above energy E):

$$I(E^*) \leq 7 \times 10^{10} / L^4 \quad \text{cm}^{-2}\text{s}^{-1}$$

$$kE^* = \frac{B^2}{2\mu_0 n(s+1)^2 s}$$

where s is a measure of the anisotropy of the pitch angle distribution function:

$$f \sim \sin^{2s} \alpha$$

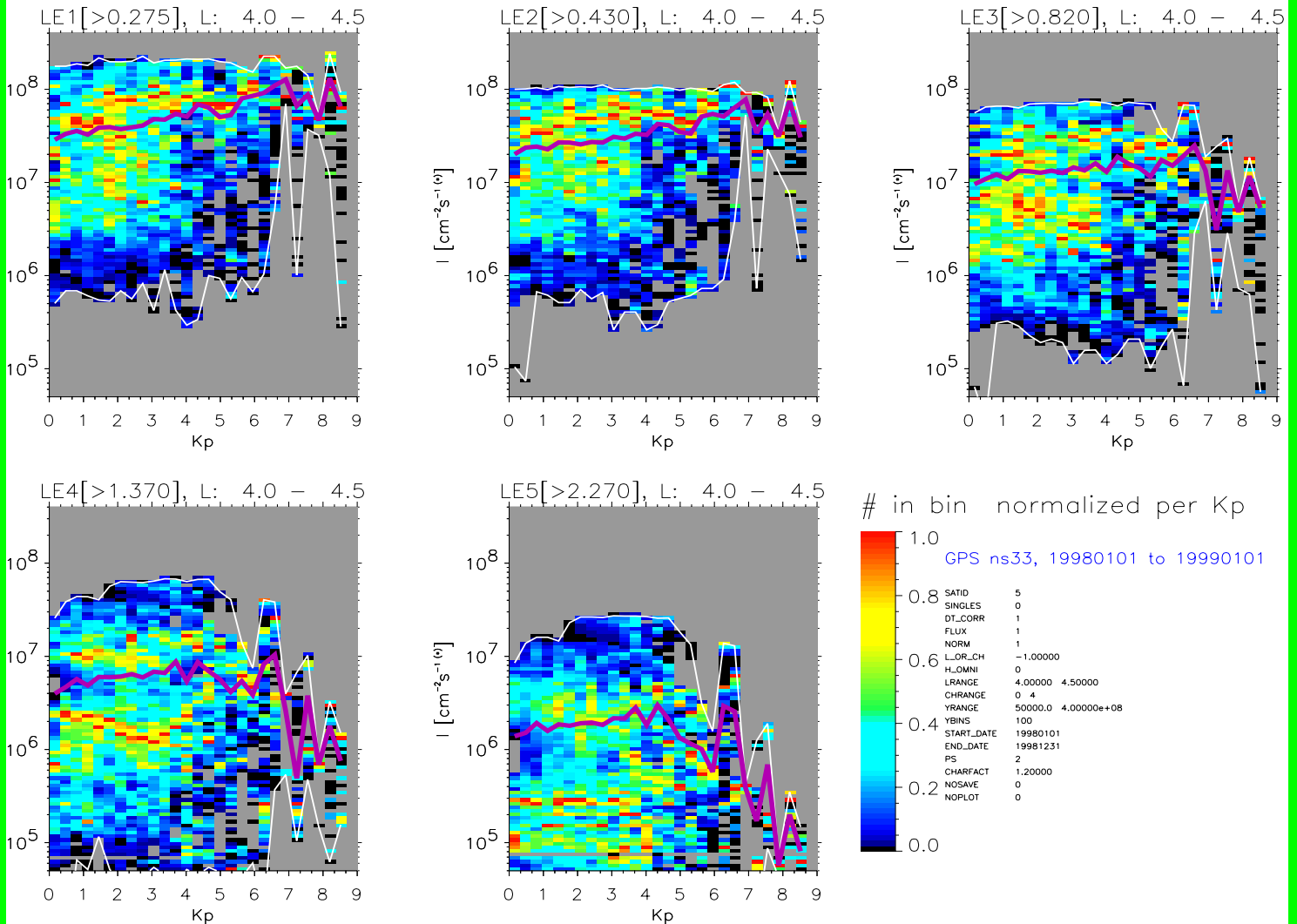
- For $L \sim 4.25$, plasma density $n \sim 5 \text{ cm}^{-3}$, and a typical value for the anisotropy index $s \sim 0.5$, with the threshold energy $E^* \sim 70 \text{ keV}$ this becomes:

$$I^* \sim 2 \times 10^8 \quad \text{cm}^{-2}\text{s}^{-1}$$

F. Observations GPS NS33, 1998, $4 < L < 4.5$



Number of data points at each flux and Kp level for the LE channels at a fixed L-range ($4 < L < 4.5$).

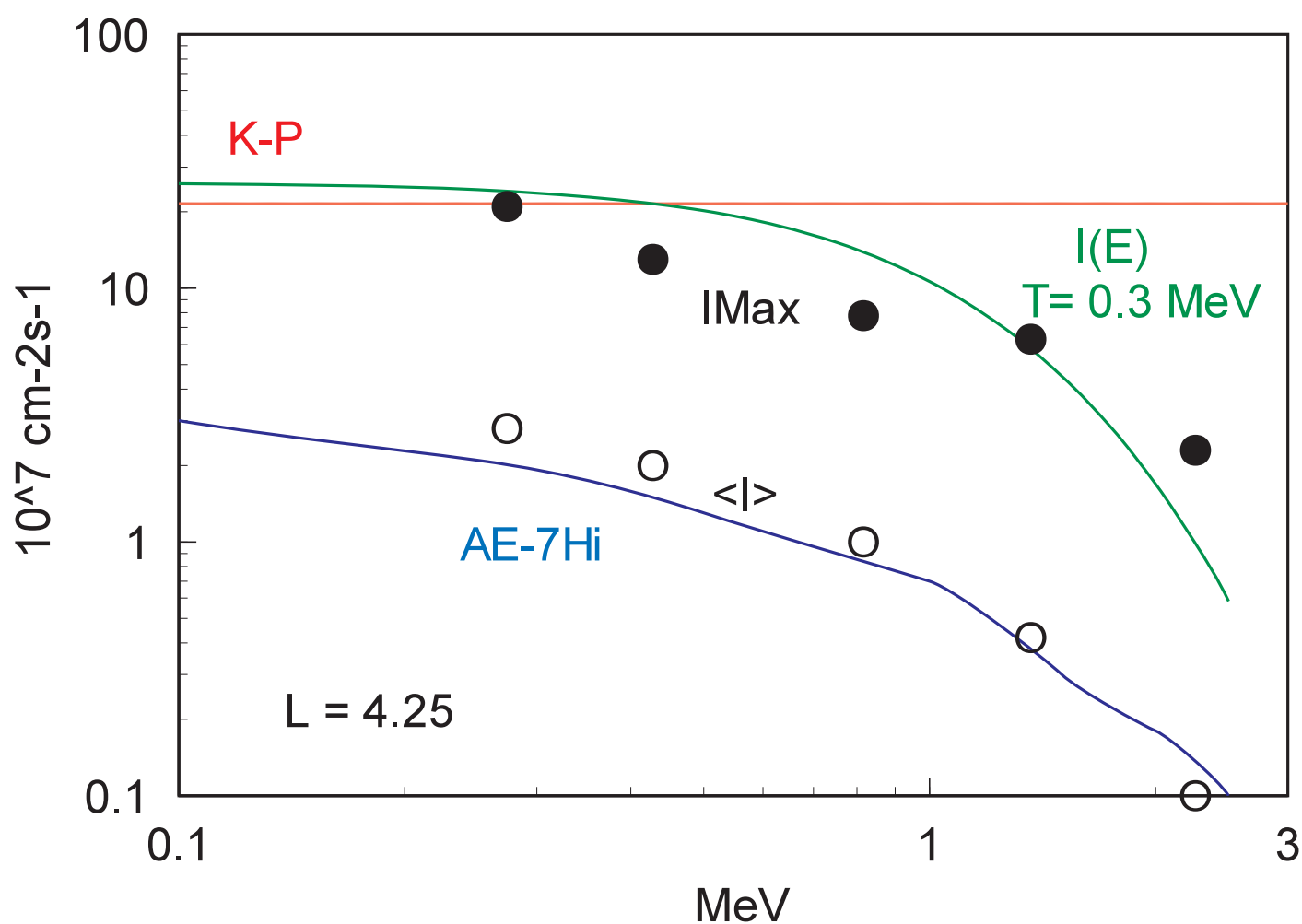


Data are normalized to the most frequently occurring flux in each Kp bin (purple curve). The white lines are the envelopes of the highest and lowest flux at each Kp.

G. Comparison of Energy Dependence



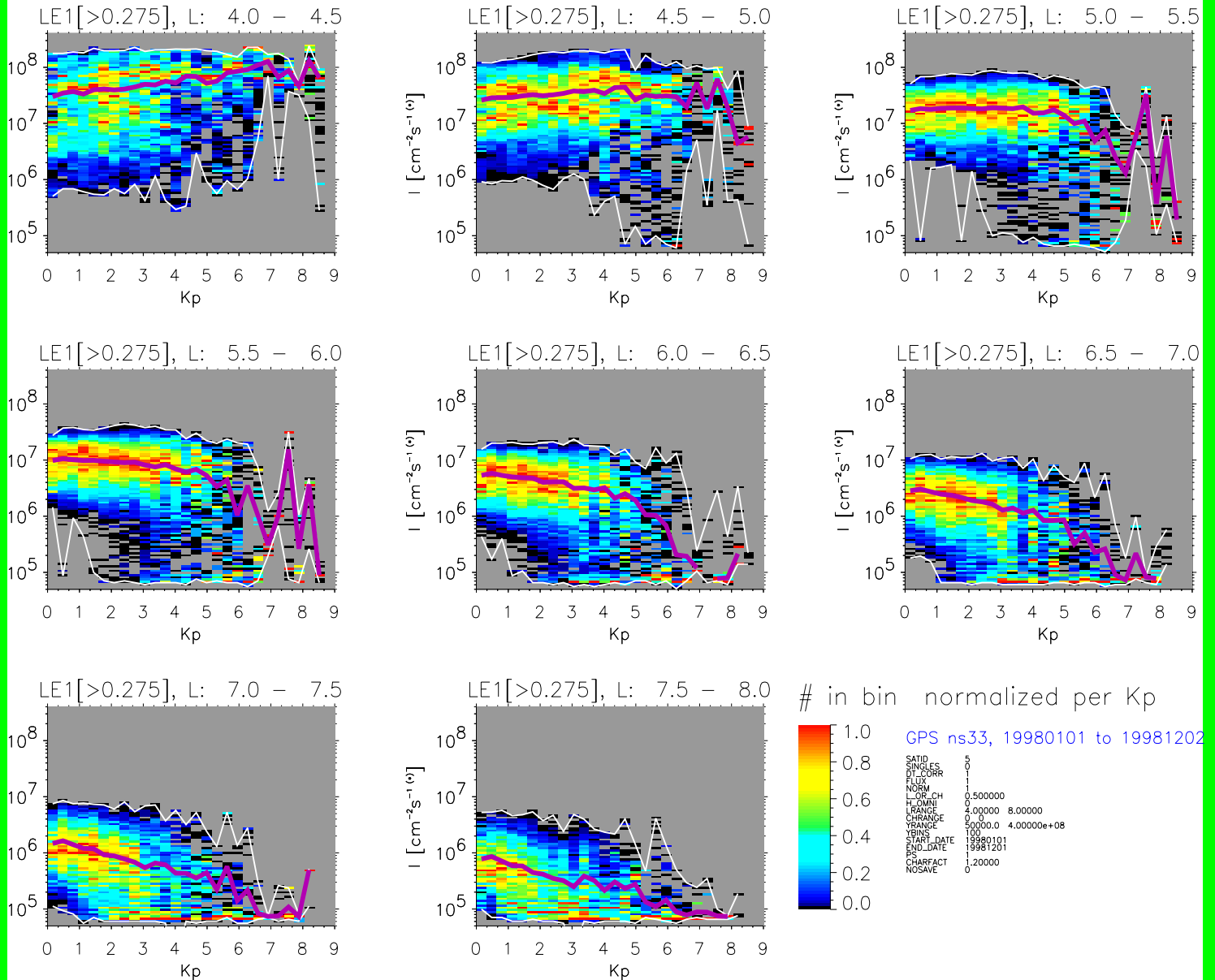
We compare here the dependence of the flux limits with energy for the theoretical Kennel & Petschek limit (K-P, in red) to the GPS observations (black, filled circles are maximum fluxes, open circles mean fluxes) and the AE7(high) model; at $L = 4.25$ (GPS on the geomagnetic equator).



H. Observations GPS NS33, 1998, LE1



Number of data points at each flux and Kp level for a range of L-values.



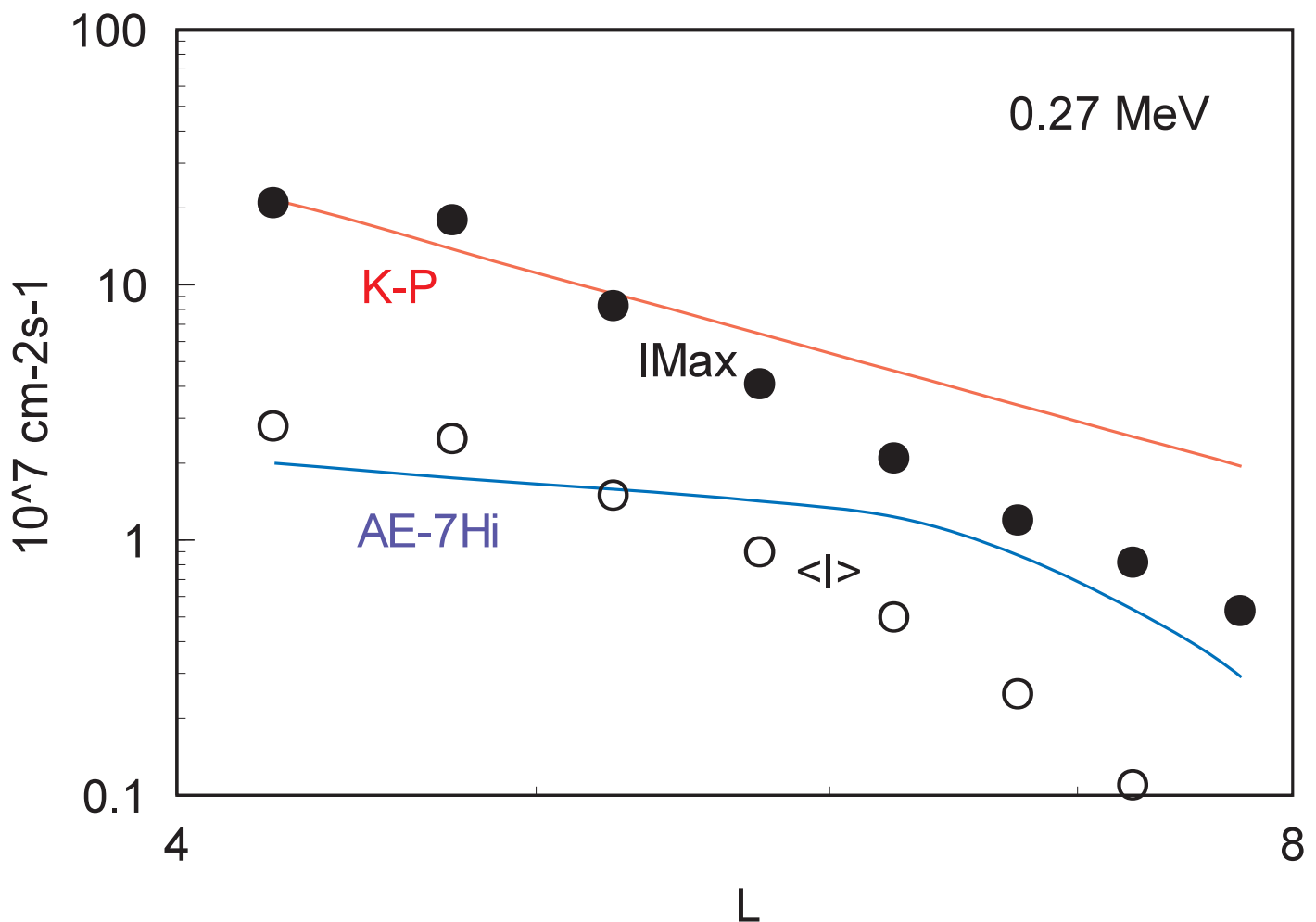
Data are normalized to the most frequently occurring flux in each Kp bin (purple curve). The white lines are the envelopes of the highest and lowest flux at each Kp.

I.1

Comparison of L Dependence Uncorrected



We compare here the dependence of the flux limits with L for the theoretical Kennel & Petschek limit (K-P, in red) to the GPS observations (black, filled circles are maximum fluxes, open circles mean fluxes) and the AE7(hi) model; for the integral channel > 0.27 MeV (LE1).



GPS latitude increases with L - data is not corrected to the equator

I.2

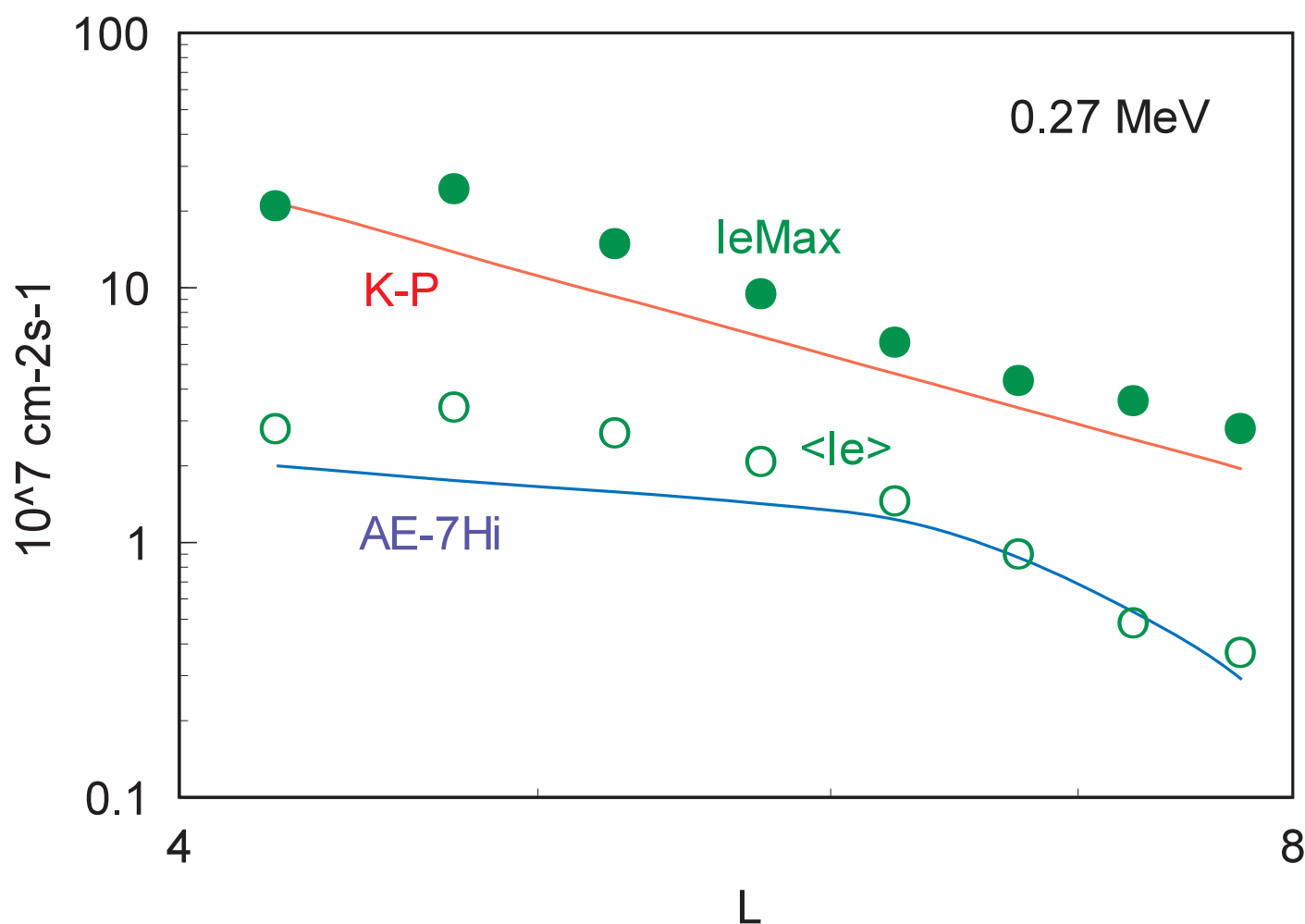
Comparison of L Dependence Corrected



To account for the lower fluxes at higher magnetic latitude we can correct to the equator:

$$J(B_e)/J(B) = (B/B_e)^s, j \sim \sin^{2s} \alpha_e \text{ and } s \sim 0.5.$$

Using a dipole & GPS orbit $(B/B_e) \sim (L/4.2)^{3.7}$, so the correction becomes $I_e \sim I(L/4.2)^{3.7s}$.



The corrected data fit both K-P and AE-7 Hi quite well.

J. Conclusions



- GPS data is becoming quantitative.
- Electron data is consistent with Kennel-Petschek flux limit ($I^* \leq 2 \times 10^8 \text{ cm}^{-2}\text{s}^{-1}$ at $L \sim 4.2$).
- Electron data is consistent with the AE-7 (High) model.
- There is little evidence for these energies of times when the maximum flux limit is exceeded (strong diffusion limit).
- The assumption of $s \sim 0.5$ for the electron pitch angle anisotropy works well for this energy range and can be used successfully to transform GPS measurements to the equatorial plane.
- Future work will include:
 - Extension of the Kennel & Petschek limit to all GPS channels.
 - Further calibration of other GPS satellite data using NS33 as a reference and using other data (POLAR HIST, CRRES MEA, HEEF) for detailed conjunction cross-calibration.
 - Detailed event analysis.